Matching mid-to-latest Carboniferous pole paths for eastern Australia and northern Armorica indicate a Pangea-B configuration and a latest Visean-Serpukhovian IITPW event

Chris Klootwijk, Research School of Earth Sciences, ANU
chris.klootwijk@anu.edu.au

TS4.2- vTE.3
EGU23-933

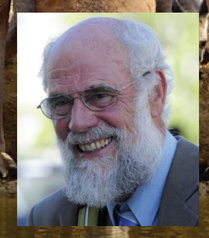

The shape of the Carboniferous pole path for Australia is disputed (Klootwijk, 2010). Conventional pole paths show compact *from-south-over-**west**-to-north* loops with western, mid Carboniferous, apices (Fig. 1a). The alternative pole path (SNEO) shows an extended *from-south-over-**east**-to-north* loop with a far-eastern, mid Carboniferous, apex (Fig. 1b). The SNEO pole path is derived from ignimbritic successions, 400 sites spanning some 50 myr, from mainly the western Tamworth Belt (Rocky Creek, Werrie, Rouchel blocks) of the southern New England Orogen (Fig. 2) (Klootwijk, 2020, 2022, 2023).

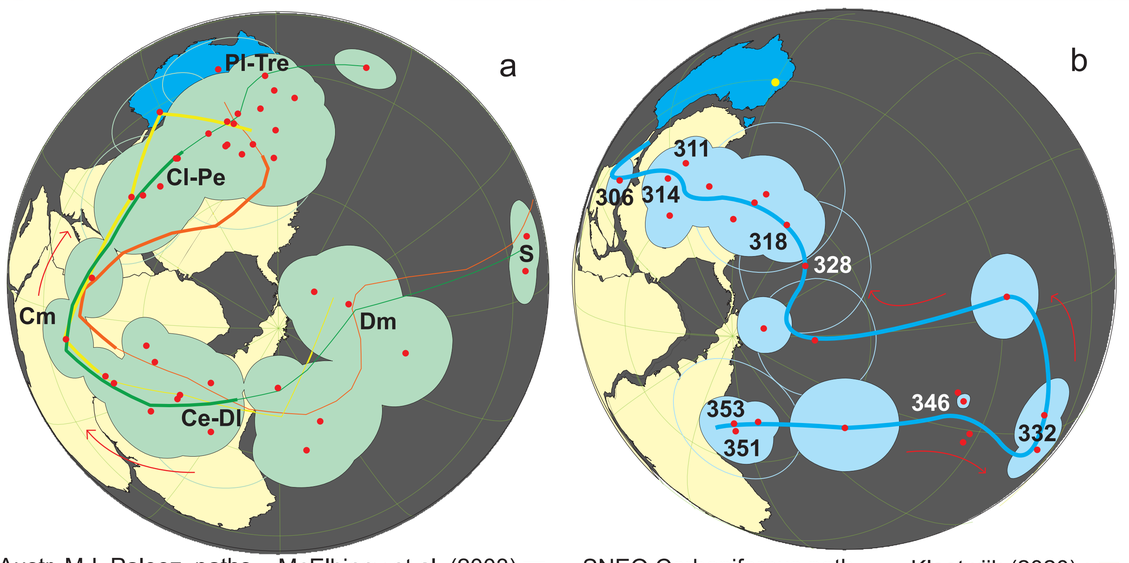

Fig. 1 (right) a) Middle-to-late Paleozoic pole paths for Australia, Carboniferous segments highlighted (Clark et al., 2003, poles shown; McElhinny et al., 2003; Anderson et al., 2004). b) Carboniferous pole path for the southern New England Orogen (SNEO, yellow dot) (Klootwijk, 2020, 2023). Ages in Ma.

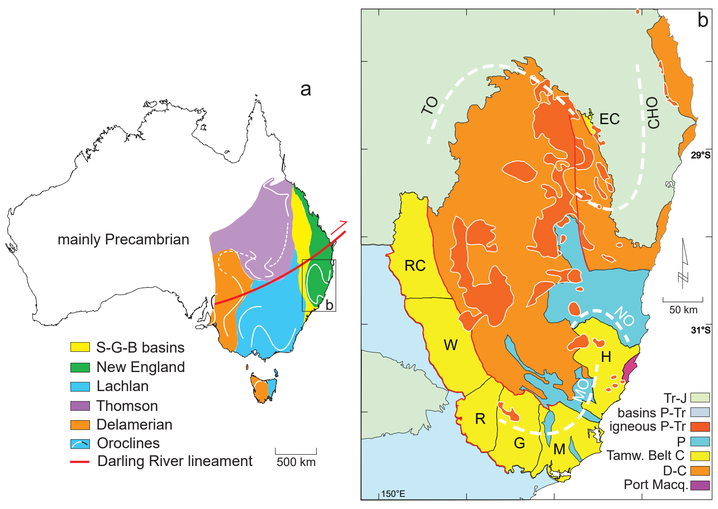

Fig. 2 Oroclinal structures of the Tasmanides (a) and SNEO (b) (Klootwijk, 2020, 2023). S-G-B basins= Sydney-Gunnedah-Bowen basin system; CHO= Coffs-Harbour Orocline; EC= Emu Creek Block; G= Gresford Block; H= Hastings blocks; M= Myall blocks; MO= Manning Orocline; NO= Nambucca Orocline; R= Rouchel Block; RC= Rocky Creek Block; TO= Texas Orocline; W= Werrie Block.

The SNEO path is thought representative for Australia and Gondwana. Legitimacy of the SNEO path is supported in showing (Klootwijk, 2023) that: (i) its extended mid-to-latest Carboniferous segment is comparable to an age-equivalent pole path segment for the northern Variscan massifs of Armorica (AR) (Fig. 3); (ii) Euler pole matching of the two mid-to-latest Carboniferous segments, taken as representatives for Gondwana (SNEO) and tentatively for Laurussia (AR), delivers a Pangea-B configuration (Fig. 4); (iii) the extended mid-to-latest Carboniferous pole path segments likely reflect a latest Visean-Serpukhovian inertial interchange true polar wander (IITPW) event (Fig. 5, 6) that led to the Serpukhovian onset of the Late Paleozoic Ice Age and the Serpukhovian biodiversity crisis (Fig. 7).

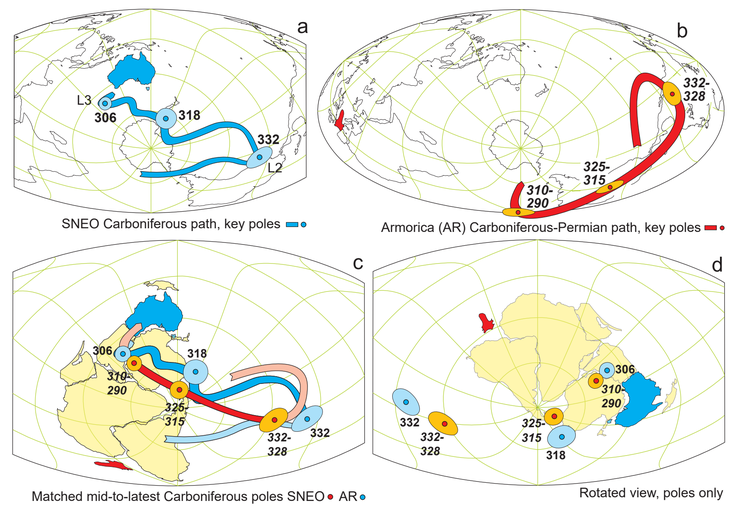

Fig. 3 a) Carboniferous SNEO pole path (Klootwijk, 2023). b) Carbonifeous-to-Permian path for Armorica (AR), after data from Edel (2001, 2003) and Edel et al. (2001, 2003). c) Euler pole matching of the mid-to-latest Carboniferous segments (highlighted) of the SNEO (a) and AR (b) paths. SNEO path taken as representative for Australia and Gondwana. Armorica relocated versus Gondwana into a Pangea-B position. d) Rotated view of (c). Ages in Ma. Matched key poles shown only.

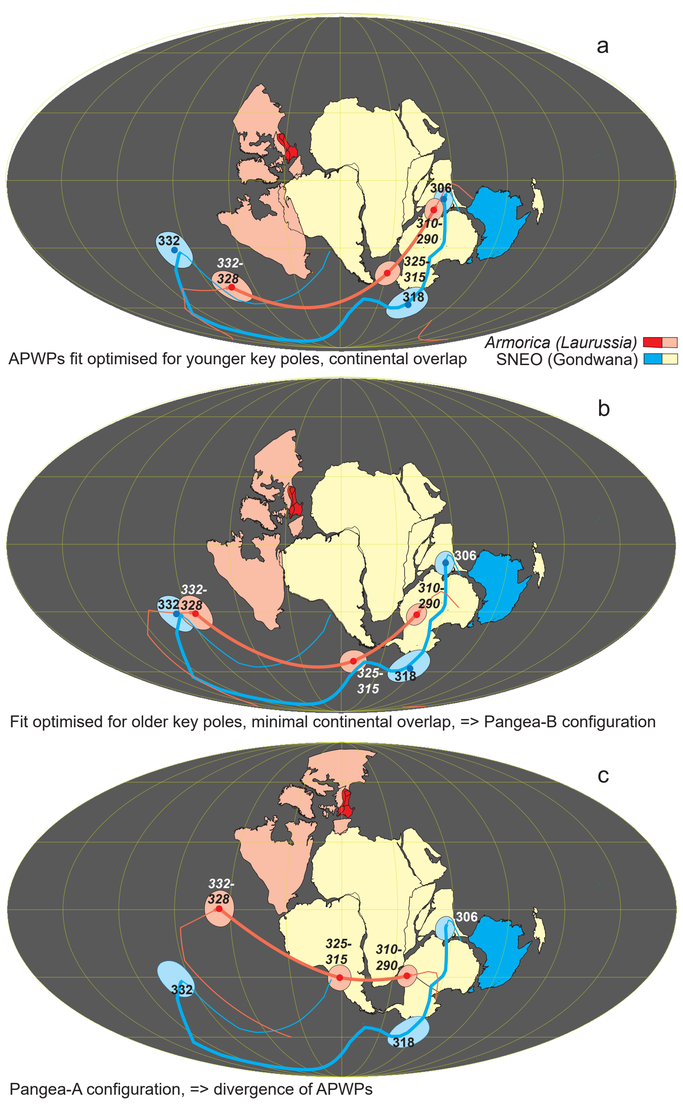

Fig. 4 Euler pole matching of mid-to-latest Carboniferous segments (highlighted) of the SNEO (Australia/Gondwana) and AR (Armorica/Laurussia) pole paths. Key poles shown only. Ages in Ma. a) Visual fit of the two sets of younger key poles, comparable to Fig. 3c, gives a Pangea-B configuration with overlap of eastern Laurentia and western South America. b) Visual fit of the set of older key poles gives a Pangea-B configuration with minimal overlap. c) A Pangea-A reconstruction (Torsvik et al., 2021) gives diverging segments, negating Pangea-A for mid-to-latest Carboniferous.

The mid-to-latest segments of the SNEO and AR paths are bounded by two substantial loops (Fig. 3, 6: L2, L3) reflecting global tectonic events and bounding existence of the Pangea-B configuration tectonically between the Sudetic and Asturian phases of the Variscan Orogeny. Changeover to Pangea-A likely started with the latest Carboniferous-earliest Permian Asturian phase, lasted till late Permian (Muttoni et al., 2019; Kent et al., 2021; Channell et al., 2022), and led to contemporaneous oroclinal deformation of the Ibero-Armorican Arc and SNEO.

Start of the Permo-Carboniferous Reverse Superchron (PCRS) (319-318 Ma, Opdyke et al., 2000; Hounslow, 2022) about coincided with ending of the latest Visean-Serpukhovian IITPW event. The IITPW event is thought triggered by a Visean northward excursion of lithospheric mass (Fig. 5c, 6b) mainly during the Sudetic phase of the Variscan Orogeny. Direct association between the IITPW event and evolution of the geodynamo into a period of very few reversals may be understandable if the African and Pacific large low shearwave provinces (LLSVPs) and associated ultra-low velocity zones (ULVZs) at the base of the mantle, rotated with the solid earth over the fluid outer core, leading to a changed core-mantle boundary heat flux, changed geodynamo-driving outer core gyrations and vastly reduced reversal rates (Biggin et al., 2012; Olson, 2016). If so, a Variscan-IITPW-PCRS causal chain would constitute an order of magnitude faster (~10^7 yr) top-down feedback between plate tectonics and the geodynamo than could be effectuated through mantle turnover.

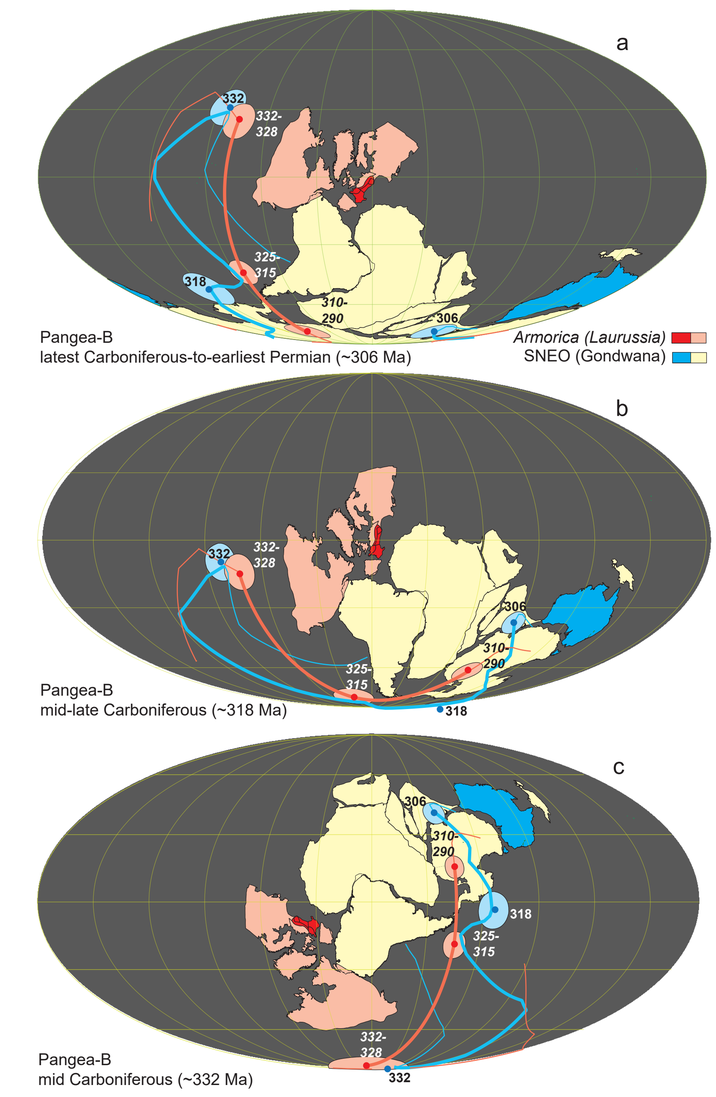

Fig. 5 Preferred Pangea-B configuration (Fig. 4b) shown in a paleomagnetic reference frame for latest Carboniferous-to-earliest Permian (a), mid-late Carboniferous (b), mid Carboniferous (c). See caption to Fig. 4. Paleolatitudinal relocations based on south pole relocation of respective means of time-corresponding key poles for the SNEO and AR pole paths. Relocations (a, b, c) demonstrate major extent of Pangea-B's mid-to-latest Carboniferous clockwise rotation: northeastern margin of Gondwana located at moderate northern latitudes in mid Carboniferous (c); Gondwana located at high and higher southern latitudes in mid-late Carboniferous (b) and latest Carboniferous-to-earliest Permian (a) respectively.

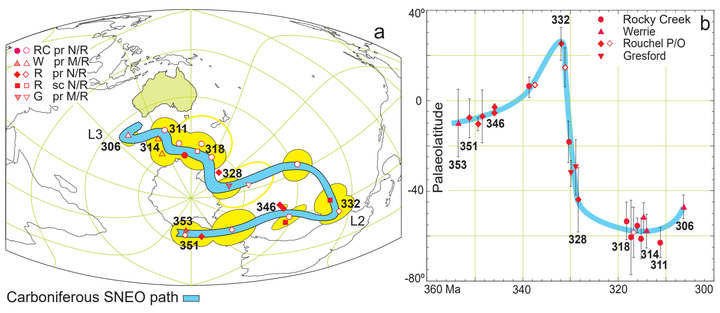

Fig. 6 Latitudinal evolution of eastern-most Gondwana (SNEO, a, b) matched by rotational evolution of western Gondwana (Armorica, c, d). a, b) Carboniferous SNEO pole path (Fig. 1b) and corresponding paleolatitudinal evolution. Ages in Ma, L2= mid Carboniferous loop, L3= latest Carboniferous-to-earliest Permian loop. c, d) Carboniferous-to-Permian pole path for Armorica (Fig. 3b [red poles], with additional poles [green] estimated from a density distribution pole path and corresponding Carboniferous rotational evolution of Armorican massifs (Edel et al., 2018; Klootwijk, 2023).

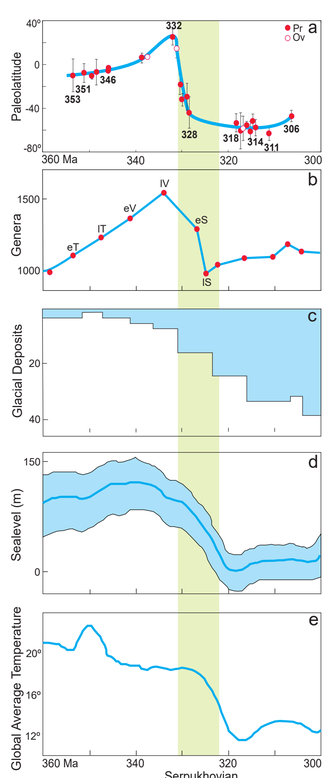

Fig. 7 (right) Carboniferous, Serpukhovian in particular, global events (b-e) versus latest Visean-Serpukhovian inertial interchange true polar wander event (a, Fig. 6b). b) Diversity of marine invertebrate genera (Stanley et al., 2003): eT= early Tournaisian; lT= late Tournaisian; eV= early Visean; lV= late Visean; eS= early Serpukhovian; lS= late Serpukhovian. c) Frequency of documented glacial deposits (Soreghan et al., 2019) as an indication of geographic extent of glacial deposits (Montañez, 2022). d) Tectono-glacio-eustatic sea level curve (van der Meer et al., 2022). e) Global average temperature curve (Scotese et al., 2021).

References
Anderson, K. L. et al., 2004. Geoph. Journ. Intern. 159, 473-485.
Biggin, A. J. et al., 2012. Nature Geosci. 5, 526-533.
Channell, J. E. T. et al., 2022. Earth-Sci. Rev. 230, 104045.
Clark, D. A. et al., 2003. Geoph. Journ. Intern. 153, 523-547.
Edel, J. B., 2001. Tectonoph. 332, 69-92.
Edel, J. B., 2003. Tectonoph. 363, 225-241.
Edel, J. B. et al., 2001. Tectonoph. 331, 145-167.
Edel, J. B. et al., 2003. Journ. Geol. Soc. Lond. 160, 209-218.
Edel, J. B. et al., 2018. Earth-Sci. Rev. 177, 589-612.
Hounslow, M. W., 2022. Geol. Soc. Lond. Spec. Publ. 512, 141-195.
Kent, D. V. et al., 2021. Gondw. Res. 92, 266-278.
Klootwijk, C., 2010. Palaeoworld 19, 174-185.
Klootwijk, C., 2020. Austral. Journ. Earth Sci. 67, 525-573.
Klootwijk, C., 2022. Austral. Journ. Earth Sci. 69, 562-590.
Klootwijk, C., 2023. Earth-Sci. Rev. Under review.
Montañez, I. P., 2022. Geol. Soc. Lond. Spec. Publ. 512, 213-245.
Muttoni, G. et al., 2019. Riv. Ital. Pal. Strat. 125, 249-269.
Olson, P., 2016. Geochem. Geophys. Geosyst. 17, 1935-1956.
Opdyke, N. D. et al., 2000. Geol. Soc. Am. Bull. 112, 1315-1341.
Scotese, C. R. et al., 2021. Earth-Sci. Rev. 213, 103503
Stanley, S. M. et al., 2003. Geology 31, 877-880.
Soreghan, G. S. et al., 2019. Geology 47, 600-604.
Torsvik, T. H. et al., 2021. Ancient Supercontinents and the Paleogeography of Earth, 577-603.
van der Meer, D. G. et al., 2022. Gondw. Res. 111, 103-121.